Clim Dyn (2013) 40:465–474
DOI 10.1007/s00382-012-1322-3

Effects of atmospheric river landfalls on the cold season precipitation in California

Jinwon Kim · Duane E. Waliser · Paul J. Neiman · Bin Guan · Ju-Mee Ryoo · Gary A. Wick

Received: 20 October 2011 / Accepted: 16 February 2012 / Published online: 3 March 2012

Abstract Effects of atmospheric river (AR) landfalls in the California coast on the cold-season precipitation in California are examined for the cold seasons of 10 water years (WYs) 2001–2010 using observed data and regional modeling in conjunction with AR-landfall inventory based on visual inspections of precipitable water vapor (PWV) from remote sensing and reanalysis. The PWV in the SSM/I and SSMIS retrievals and the ERA-Interim reanalysis shows 95 AR-landfall days in the California coast that are almost evenly split between the northern and southern coasts across 37.5N. The CPC/NCEP gridded daily precipitation analysis shows that 10–30% of the cold-season precipitation totals in California have occurred during these AR landfalls. The analysis also reveals that the percentage of precipitation and the precipitation intensity during AR landfalls in California are characterized by strong north-to-south gradient. This north–south contrast in the AR precipitation is reversed for the non-AR precipitation in the coastal range. The frequency of AR landfalls and the cold-season precipitation totals in the Sierra Nevada region are only marginally correlated. Instead, AR landfalls are closely related with the occurrence of heavy precipitation events. The freezing-level altitudes are systematically higher for AR wet days than non-AR wet days indicating warmer low-troposphere during AR storms. Cold season simulations for the 10 WYs 2001–2010 show that the Weather Research and Forecast (WRF) model can reasonably simulate important features in both the seasonal and AR precipitation totals. The daily pattern correlation coefficients between the simulated and ERA-Interim upper-air fields exceed 0.9 for most of the period. This suggests that the simulated temporal variations in the atmospheric circulation agree reasonably with the reanalysis over seasonal time scales, characteristics critical for reliable simulations of regional scale hydrologic cycle. The simulated seasonal and AR precipitation totals also agree reasonably with the CPC/NCEP precipitation analysis. The most notable model errors include the overestimation (underestimation) of the season-total and AR precipitation in the northern (southern) California region. The differences in the freezing-level altitudes during the AR- and non-AR wet days in the simulation agree with those from the ERA-Interim reanalysis. The freezing level altitudes are systematically overestimated in the simulations, suggesting warm biases in the low troposphere. Overall, WRF appears to perform reasonably in simulating the key features in the cold season precipitation related with AR landfalls, an important capability for assessing the impact of global climate variations and change on future hydrology in California.

Keywords Atmospheric river · AR landfall in California coast · Cold season California precipitation · Freezing level altitude

J. Kim (✉) · D. E. Waliser
University of California Los Angeles, Los Angeles, CA, USA
e-mail: jkim@atmos.ucla.edu

D. E. Waliser · B. Guan · J.-M. Ryoo
Jet Propulsion Laboratory, California Institute of Technology, Pasadena, CA, USA

P. J. Neiman · G. A. Wick
Earth System Research Laboratory, NOAA, Boulder, CO, USA

Present Address:
J.-M. Ryoo
University of California Berkeley, Berkeley, CA, USA

1 Introduction

Atmospheric Rivers (ARs) are a region of deep corridor of intense moisture transport over oceans often found in the

warm sector of extratropical cyclones that transport moisture from lower latitudes, including the tropics in some events, to higher latitudes (Neiman et al. 2008a; Ralph et al. 2004, 2006; Zhu and Newell 1994). It has been found that over 90% of the poleward atmospheric moisture transport is carried by ARs within 10% of the zonal circumference at midlatitudes (Zhu and Newell 1998; Neiman et al. 2008a, b). Bao et al. (2006) and Knippertz and Wernli (2010) show that some of the moisture is directly from the tropics. A Lagrangian air-parcel trajectory study of Ryoo et al. (2010) shows that most AR storms are characterized by southwesterly paths with possible links with the tropics. ARs are characterized by narrow and elongated regions of intense water vapor fluxes with large moisture contents and weak moist static stability in the low troposphere (Ralph et al. 2005), a condition ready for producing heavy precipitation when the inflow is subject to orographic lifting. Thus, AR landfalls in the regions of hilly terrain such as California's coastal range and the Sierra Nevada often bring heavy precipitation accompanied by extreme streamflow events.

ARs are of a particular importance in California's mountainous coastal and the Sierra Nevada regions. AR landfalls have been related with extreme precipitation and flooding in California's mountainous regions (Ralph et al. 2006; Neiman et al. 2008b; Leung and Qian 2009; Soong and Kim 1996). In addition, much of the cold season precipitation in California occurs in a relatively small number of intense storms (Kim 1997). A number of these intense events are associated with AR landfalls (Dettinger et al. 2011), especially those traditionally called pineapple express storms that often show moisture paths extending from the subtropical Pacific Ocean near Hawaii to the west coast of the United States (US) (Dettinger 2004). Thus AR landfalls are an important topic related with climate variations and change as heavy precipitation, snowfall, and snowpack directly affect water resources and flooding in California.

There exist only a limited number of studies on the impact of ARs on the precipitation in California. Although the term AR was first introduced in early 1990s (Zhu and Newell 1994), ARs have become visualized only recently via satellite-retrieved precipitable water vapor (PWV) field (Ralph et al. 2004; Neiman et al. 2008a, b). Because of this, much of the details on the relationship between ARs and the regional precipitation remain to be explored. The recent study by Dettinger et al. (2011) investigates AR precipitation for all AR landfalls along the entire US west coast. As individual ARs affect only limited meridional extents of a few hundred kilometers, their results may not be suitable for representing the relationship between AR landfalls and precipitation in California. Unlike the previous one, this study documents the precipitation characteristics in California associated only with the AR landfalls in the California coast. The more localized relationship between AR landfalls and precipitation is fundamental for future studies on the AR-related water cycle and the mesoscale processes behind the regional circulation and precipitation distribution in California, especially by orographic forcing (e.g., Kim and Kang 2007).

Assessing the impacts of global climate variations and change on regional sectors has become an important research topic for supporting decision makers in developing the plans for adapting to and mitigating the effects of future climate change on important sectors. Regional climate modeling is a key in these impact assessment studies as they are the only means to obtain multiple climate variables that can preserve dynamical and physical consistency with the global model data as well as among the downscaled variables (e.g., Giorgi et al. 1997; Kim et al. 2002; Kim and Lee 2003). Among the key concerns in regional climate modeling for climate forecasts and projections is the performance of the model in simulating important features in the regional water cycle. Hence, model evaluation has become a key part of climate projection and impact assessment studies (Nature 2010). Because AR can be a major factor that affects the water cycle in California, evaluating a regional climate model in simulating AR-related precipitation is an important step before seasonal climate prediction studies and/or climate change experiments. The analysis of observed and reanalysis data in the first part this study are designed to examine the AR-related precipitation and freezing-level characteristics for exactly the same period as the model simulations so that results in the analysis work can be directly relevant for the model evaluation study in the second part of the paper.

This study documents the climatology of the cold season precipitation and freezing-level altitudes during AR landfalls along the California coast for the cold 10 WYs 2001–2010 by analyzing gridded daily precipitation data and reanalysis. The observed climatology is in turn used to evaluate results from a seasonal hindcast experiment using the WRF Model in order to examine its performance in simulating AR-related cold season hydrology in California in preparation for future experiments on seasonal forecasting and climate change projections for California. This paper is organized as follow. Sections 2 and 3 present the precipitation and freezing-level climatology from the Climate Prediction Center/National Centers for Environmental Prediction (CPC/NCEP) daily rain gauge analysis data and the ERA-Interim reanalysis data (Simmons et al. 2006), respectively, over the 10 cold seasons. Section 4 presents the evaluation of the simulated cold season precipitation and freezing level altitudes against the observed climatology obtained in Sects. 2 and 3. Conclusions and discussions are presented in Sect. 5.

2 Data

The 0.25°-resolution gridded daily rain gauge analysis by the National Centers for Environmental Prediction (NCEP) Climate Prediction Center (CPC) (Higgins et al. 2000) is used to calculate the daily precipitation characteristics in California. A total of 95 AR landfalls in the California coast 32.5N–41N (Neiman et al. 2008b) are identified for the cold season (October–March) of the 10 water years (WYs) 2001–2010 using the method by Neiman et al. (2008b) based on using the satellite-retrieved (SSM/I and SSMIS) PWV as a proxy for AR detection. It defines ARs as 'narrow plumes of SSM/I PWV with values >20 mm that are >2,000-km long and <1,000-km wide'. This PWV structure associated with ARs also appears clearly in the ERA-Interim reanalysis. Because the satellite-based AR inventory does not distinguish the landfalls in the northern California coast from those in the southern California coast, the ERA-Interim reanalysis are used to regroup the 95 AR landfalls into the northern and southern groups with respect to 37.5N. Firstly, the reanalysis PWV fields at 12 UTC on the 95 landfalls are plotted. Then, the AR landfalls are counted towards two groups to the north and south of 37.5N. If a PWV plume makes a landfall across 37.5N, it is double-counted into the two groups. The results show that the 95 AR landfalls are almost evenly split between the northern and southern coasts. A grouping based on the 00UTC field results in a similar number. The reanalysis data are also used to calculate the freezing level altitudes. The Sierra Nevada region is divided into the northern (NSN) and southern (SSN) regions with respect to 37.5N (Fig. 1b) for analysis.

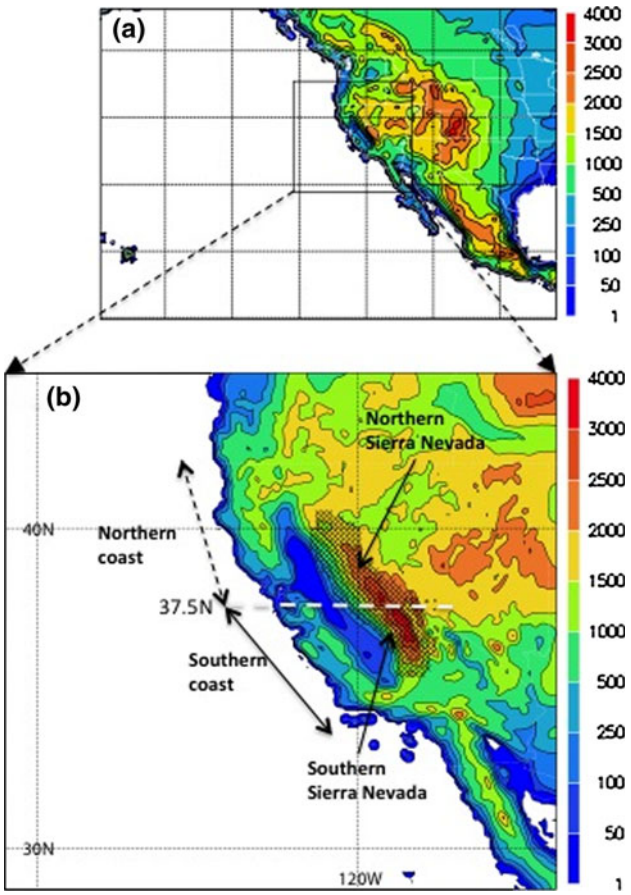

Fig. 1 The model domain and orography for the (**a**) coarse- and (**b**) fine-resolution domains. *Shading* in **b** indicates the Sierra Nevada region. The lines off the coast of California in **b** indicates the extent of the California coast line defined as the northern and southern California coasts in classifying the AR landfalls into the northern and southern groups

3 Observed precipitation and freezing level altitudes

3.1 Cold season precipitation and ARs

The cold-season mean precipitation (Fig. 2a) shows the well-known orographic effects with precipitation maxima in high elevations (Kim 1997; Kim and Lee 2003). The AR-precipitation totals (Fig. 2b) show similar geographical distribution as the season totals (Fig. 2a), but with smaller contrasts between the coastal range and the Central Valley. The AR precipitation ranges from 10 to 30% of the season total and is characterized by notable contrasts between the northern and southern California regions (Fig. 2c). To the north of the San Francisco Bay, 20–30% of the season-total precipitation fell during AR events, but <15% is related with ARs to the south of the Monterey Bay. Thus, AR landfalls affect northern California more than the southern region perhaps because the winter storm track is more active, on average, in the northern half of the state and/or orographic blocking generates southerly moisture transport upstream of the major mountain ranges (Kim and Kang 2007). Details on the mechanisms behind the north–south gradient are a subject of future studies, especially in relationship with long-term climate variations.

3.2 Wet-day precipitation

Wet-day mean precipitation (Fig. 3a), an indicator for the daily precipitation intensity, is similar to the season totals (Fig. 2a), re-affirming the importance of the orographic effects. Wet days are defined using a threshold value of 0.1 mm/day in this study. Compared to the all wet days (Fig. 2a), the AR days (Fig. 3b) show stronger (weaker) intensities in the northern (southern) California region. The north–south variation in the precipitation intensity on the non-AR wet days (Fig. 3c) is much smaller than for the AR days. Also note that the precipitation intensity in the southern coastal range is smaller for the AR days than the non-AR days (Figs. 3b, 3c). Thus, AR landfalls in the California coast more

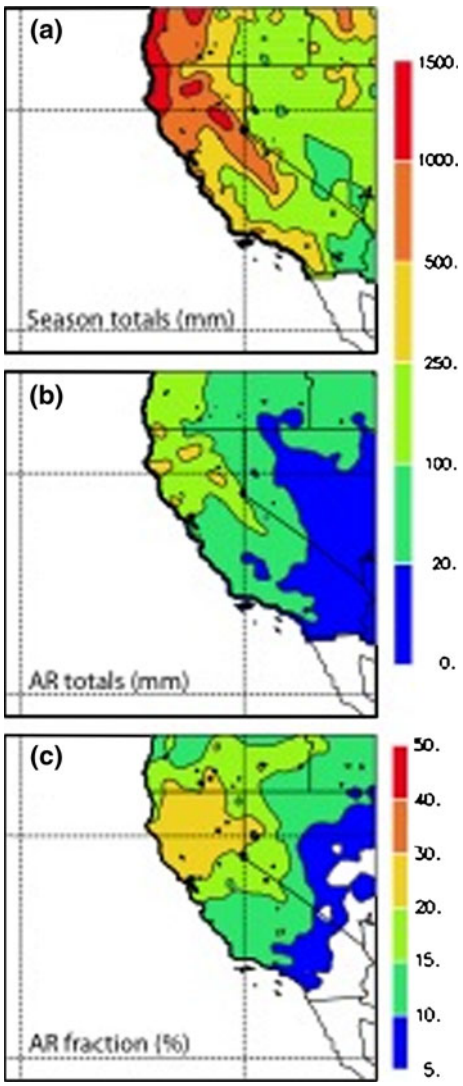

Fig. 2 The observed cold season (October–March) precipitation climatology in California for the 10 cold seasons: **a** cold-season total (mm), **b** AR-total (mm), and **c** the percentage of the cold season precipitation totals that occurred during AR events

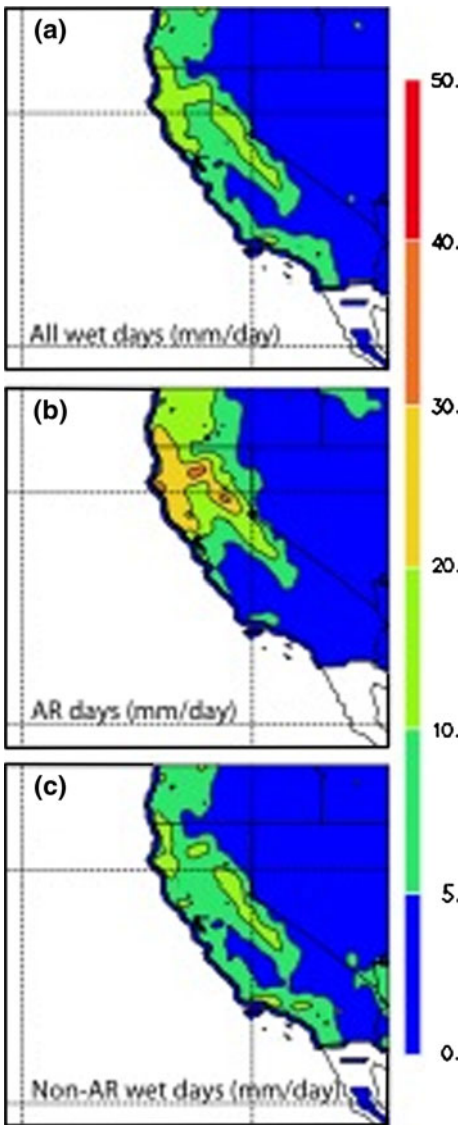

Fig. 3 The observed wet-day precipitation intensity for: **a** All wet days, **b** AR days, and **c** non-AR days

strongly affect precipitation in the northern California region than in the southern California region.

3.3 Precipitation in the Sierra Nevada region

Among the 95 AR landfall totals in the 10 cold seasons for WYs 2001–2010, noticeable (>0.1 mm/day) precipitation has occurred in 87 and 60 days for the Northern Sierra Nevada (NSN) and Southern Sierra Nevada (SSN) regions, respectively (Table 1). Thus, AR landfalls in the California coast and the occurrence of precipitation are more closely related in the NSN region than the SSN region. In this section, the AR effects on precipitation and low-level temperatures are examined for three Sierra Nevada regions (All SN, NSN and SSN in Fig. 4).

The number of AR landfalls in a cold season undergoes large interannual variations, 1–15 per year, with a 10-season average of 9.4 landfalls per year (Fig. 4). The number of ARs and the cold season precipitation totals are only marginally related, with the correlation coefficients of 0.57 and 0.44 for NSN and SSN, respectively (Fig. 4a). AR precipitation is more closely correlated with the number of AR landfalls with the correlation coefficients of 0.85 for NSN and 0.56 for SSN (Fig. 4b). Thus the AR precipitation amounts are more closely correlated with the number of AR landfalls in the NSN than in the SSN. This suggests that the NSN receives more direct impacts than the southern region similarly as the precipitation intensity shown in Fig. 3. Interannual precipitation variations for the entire Sierra Nevada region (All SN in Fig. 4a, b) resemble

Table 1 The mean freezing altitudes (meters) over the NSN and SSN regions during AR- and non-AR precipitation events for the 10 cold seasons calculated from the ERA-Interim reanalysis data and model simulations

	NSN		SSN	
	ERA-Interim	WRF	ERA-Interim	WRF
AR wet days	2,746 m (87)	3,025 m (74)	2,949 m (60)	3,314 m (50)
Non-AR wet days	2,332 m (792)	2,753 m (698)	2,428 m (603)	2,998 m (455)
Differences	414 m	272 m	521 m	316 m

The numbers in the parenthesis are the number of AR- and non-AR wet days in the 10 WYs. The wet days are defined with the threshold precipitation value of 0.1 mm/day

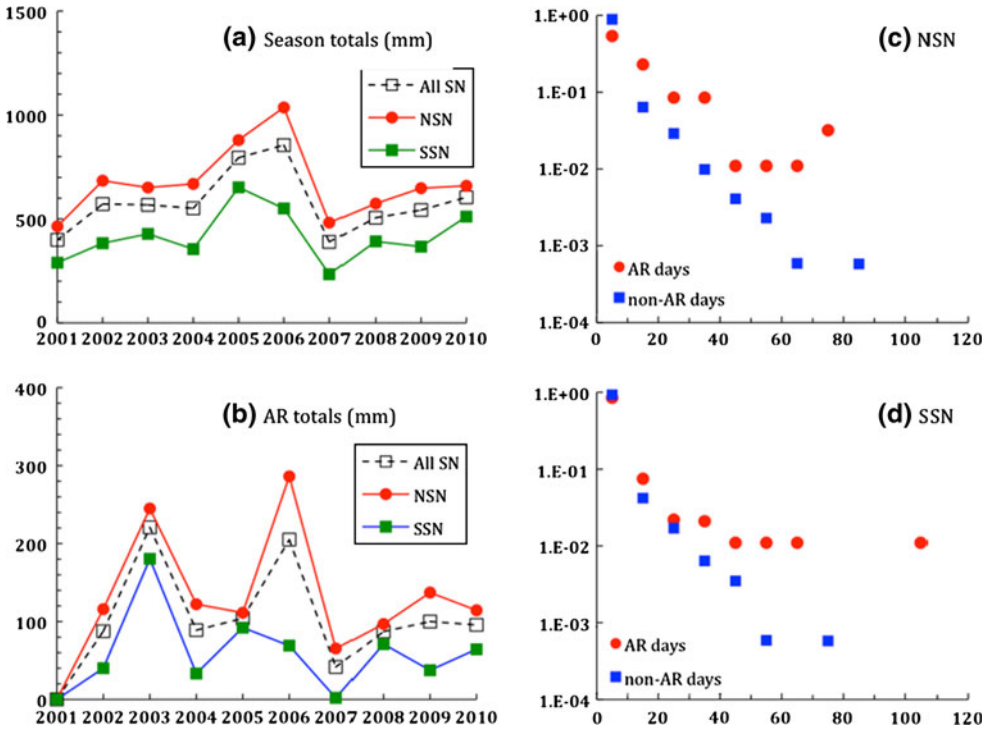

Fig. 4 The annual precipitation (mm) in the three Sierra Nevada regions (*lines with symbols*) and the number of AR events (*blue numbers*) for the 10 WYs 2001–2010. The figures on the *right hand side* are the PDFs of daily precipitation for the two Sierra Nevada regions: **c** NSN, and **d** SSN

more closely that for the NSN region because the northern region receives more precipitation than the southern region.

The probability distribution functions (PDFs) of the wet-day precipitation intensity over the two Sierra Nevada regions (Fig. 4c, d) show that AR landfalls are closely related with the occurrence of heavy precipitation events in all three Sierra Nevada regions. Note that the heaviest precipitation event in the NSN region for non-AR days (Fig. 4c) is contributed from a single event during the 10 cold seasons. Thus, AR landfalls are more closely related with heavy precipitation events than the season totals. Again, the precipitation intensity PDFs for the entire Sierra Nevada region resembles that of the NSN region.

3.4 Freezing level altitudes

Freezing-level altitudes are directly related with two important hydrologic processes, snowmelt and the partitioning of precipitation between rainfall and snowfall, and are often used as the surrogate for snowline during precipitation. Calculations using the ERA-Interim reanalysis show that freezing level altitudes are higher during the AR storms than the non-AR storms in both Sierra Nevada regions systematically over the entire 10 cold seasons. The differences in the freezing-level altitudes for the 10 cold seasons are 497 and 843 m for NSN and SSN (Table 1). This in turn shows that the low-level temperatures during AR storms are higher than those during the non-AR storms by 5–8 K. This is consistent with Neiman et al. (2008b) who found that the AR storms are characterized by warmer low troposphere than the non-AR storms during cold seasons. This shows that the warmer and stronger storms during AR landfalls can substantially increase flood potential not only via heavy precipitation but also via the possibility of inducing a large amount of snowmelt during precipitation.

4 Cold season WRF hindcast

In preparation for extended-range (seasonal, interannual, and decadal) predictions of cold season hydrology in California and regional climate projections for climate-change impact assessment studies using the dynamical downscaling method, the precipitation and freezing level simulated in the WRF model hindcast are evaluated in the following sections. The observed variations in the cold season precipitation and freezing-level altitudes in relationship with AR landfalls obtained in the previous sections are used as the reference for the model evaluation study. Details of the numerical experiment and evaluation are presented in the sub-sections below.

4.1 Numerical experiment

The WRF model v3.1.1 has been used to simulate the cold season climate in California in a one-way nested model domain. The outer domain (Fig. 1a) covers the Eastern North Pacific and the western US at a 0.36° horizontal resolution and the inner domain (Fig. 1b) covers California at a 0.09° horizontal resolution. Also shown in Fig. 1b are the geographical references used to define the northern and southern California regions. Both domains are discretized vertically with 27 layers. The model physics used in this study include the YSU PBL, Kain-Frisch convection, WSM 5-class microphysics, NOAH land surface, RRTM longwave and Dudhia shortwave schemes. For more details of the WRF model and available physics modules, readers are referred to Skamarock et al. (2008) and http://www.mmm.ucar.edu/wrf/users/wrfv3.1/updates-3.1.1.html. We have performed cold season (October–March) simulations for the 10 WYs 2001–2010. The large-scale forcing data have been constructed from the ERA-Interim reanalysis data at 6-h intervals using the WRF Preprocessing System distributed with WRF.

4.2 Upper-air fields

The daily time series of the spatial pattern correlation between the simulated and reanalysis temperatures and geopotential heights at the 700 and 300 hPa levels as well as PWV are examined to evaluate the performance of the regional model in simulating the large-scale circulation over the Eastern Pacific. The spatial pattern correlation coefficients in Fig. 5 are calculated for the 00UTC fields; calculations for the 12UTC fields yield essentially the same results. The quality of the simulated upper-air fields over the Eastern Pacific is a precondition for reliable simulations of mesoscale circulation and hydrology in California (Kim and Lee 2003). The simulated upper-air fields (Fig. 5a, b) remain reasonably close with those depicted in the ERA-Interim reanalysis with the correlation coefficients exceeding 0.9 for most of the days for both

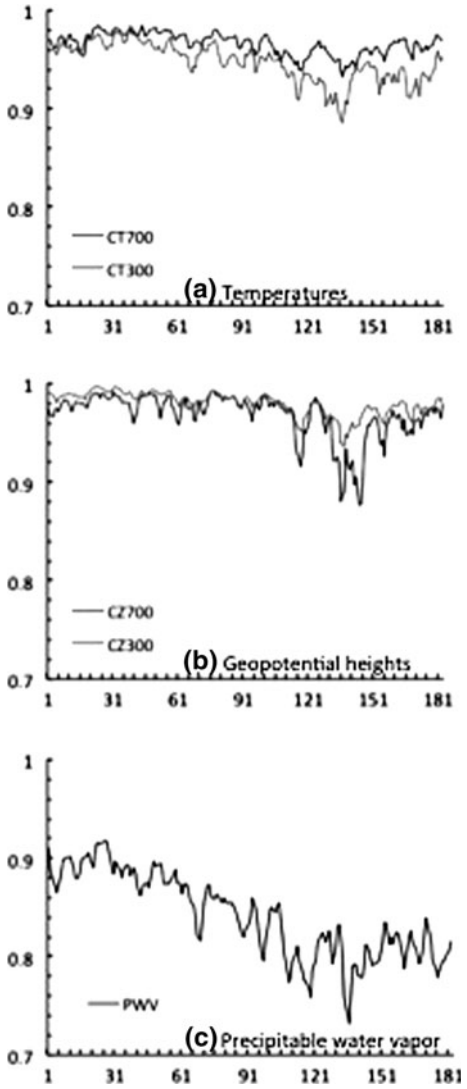

Fig. 5 The daily pattern correlation coefficients between the simulation and the ERA-Interim reanalysis averaged over the 10 cold seasons: **a** temperatures at the 700 hPa (CT700) and 300 hPa (CT300) levels, **b** geopotential heights at the 700 hPa (CT700) and 300 hPa (CT300) levels and **c** precipitable water vapor

fields at both levels. The correlation coefficients deteriorate in the mid- to late February period (between the days 130 and 140 from October 1), but recover in March. The spatial correlation coefficients for PWV between the simulation and the reanalysis (Fig. 5c) are smaller than either temperatures or geopotential heights; however, they remain above 0.8 for most of the cold season. This suggests that the WRF model has simulated key features in the large-scale circulation during the course of the cold season with reasonable accuracy.

4.3 Cold-season precipitation

The model simulates well the spatial variations in the cold season precipitation in the region characterized by the

heaviest precipitation in the coastal regions of northern California and Oregon, heavy orographic precipitation in the Sierra Nevada region, rain shadows in the Central Valley and to the east of the Sierra Nevada, and the north–south precipitation gradient (Fig. 6a). The simulation also depicts the north–south contrast in the effects of AR landfalls on precipitation, in amounts and the percentage of the season total (Fig. 6b, c). Compared to the CPC data (Fig. 2a), the most notable bias in the simulated precipitation is the general overestimation (underestimation) of precipitation in northern (southern) California. Especially, the simulation substantially underestimates the heavy precipitation in the southern coastal range. The simulation also overestimates the percentage of AR precipitation in the central California region.

The simulated wet-day (Fig. 7a) and AR-day (Fig. 7b) precipitation intensity agrees well with those from the CPC data shown in Fig. 3a, b, respectively. The simulation also generates the non-AR mean precipitation intensity in the northern California region, but underestimates it in the southern California coastal range and overestimates in the SSN (Fig. 7c). These biases in the southern coastal range and the SSN region may be caused by the inability of the model in simulating the effects of the narrow but significant mountain ranges along the southern California coast even at quite fine sub-10 km spatial resolutions.

The interannual variations in the simulated cold-season precipitation totals agree well with observations in both NSN and SSN regions (Fig. 8a, b). The model generally overestimates (underestimates) the season-total precipitation in the NSN (SSN) region. The simulated precipitation

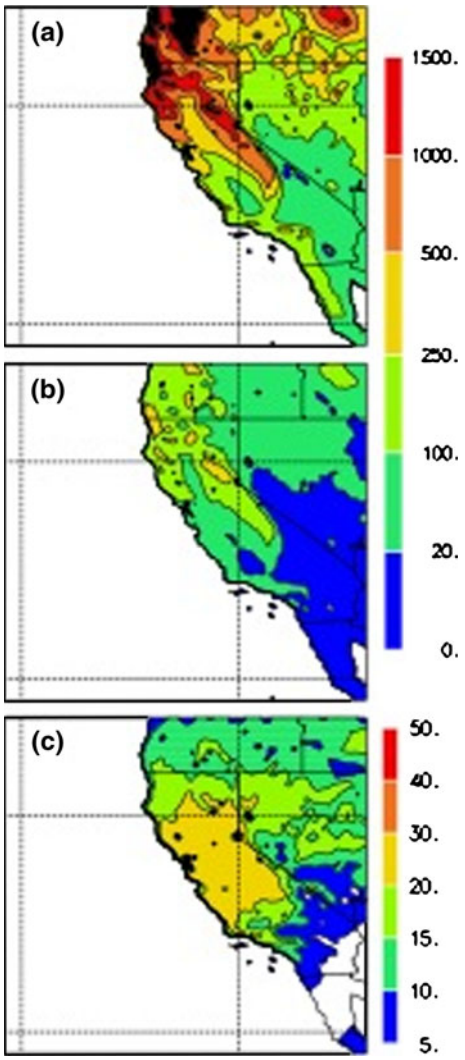

Fig. 6 The simulated cold season (October–March) precipitation climatology in California for the 10 cold seasons: **a** cold-season total (mm), **b** AR-total (mm), and **c** the percentage of the cold season precipitation totals that occurred during AR events

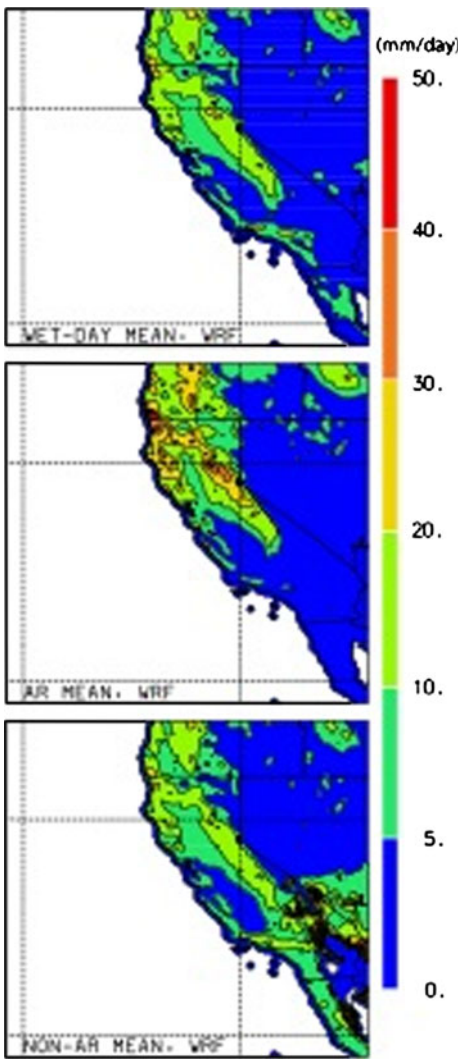

Fig. 7 The simulated wet-day precipitation intensity for: **a** all wet days, **b** AR days, and **c** non-AR days

is within 20% of the observed value in the NSN region except for the WYs 2010 and 2005 in which the model overestimates precipitation by 48 and 38% of the observed value. The model errors for the SSN region are similar, with the largest model error of 50% of the observed value in WY2001. The model also generates the observed shape of the interannual variations for both regions. The AR-total precipitation is generally overestimated in both Sierra Nevada regions (Fig. 8c, d). Compared to the season-total precipitation, the model errors in simulating the AR-total precipitation are larger; however, the simulated interannual variation agrees well with the observation.

The seasonal simulations (Fig. 9) closely represent the observed effects of AR landfalls on the PDF of daily precipitation intensity in the two Sierra Nevada regions. Like in the observations (Fig. 4c, d), AR landfalls are related with higher frequency for all precipitation intensity except the weakest daily precipitation events for both NSN and SSN regions. This implies that WRF possesses useful skill for simulating extreme hydrologic events associated with AR landfalls, an important capability for assessing the flood frequency in extended-range forecasting and regional climate projections.

4.4 Freezing-level altitudes

The simulated mean freezing level altitudes over the NSN and SSN regions during the AR- and non-AR wet days are compared against those calculated from the reanalysis data in Table 1. The simulation generally overestimates the freezing level altitudes for both regions by 300–500 m, with the largest bias over the SSN regions during non-AR wet days. The simulation also underestimates the wet days for both regions and for both AR- and non-AR days. Despite these model biases, the simulation also shows that the freezing-level altitudes are higher during AR wet days than non-AR wet days. This shows that the WRF model can simulate the differences in the low tropospheric temperatures, however, only qualitatively.

5 Conclusions and discussions

The effects of ARs on the precipitation and freezing-level altitudes in California during cold seasons (October–March) are analyzed for the 10 WYs 2001–2010. About 10-30% of cold season precipitation totals is found to be associated with AR landfalls. This is somewhat smaller than that in Dettinger et al. (2011) who estimated about 31–36% of precipitation, with a peak of 46%, at most the cooperative weather stations in Central and Northern California are from AR storms. This difference between the two studies, despite the fact that both studies are based on the same AR landfall inventory, may originate from the differences in defining 'AR precipitation' between the two studies. Dettinger et al. (2011) define AR precipitation over 2 days including a concurrent- and the following day to count the cases in which AR landfall starts on the concurrent day and ends in the following day. Unlike theirs, this study accounts precipitation only on the days of AR

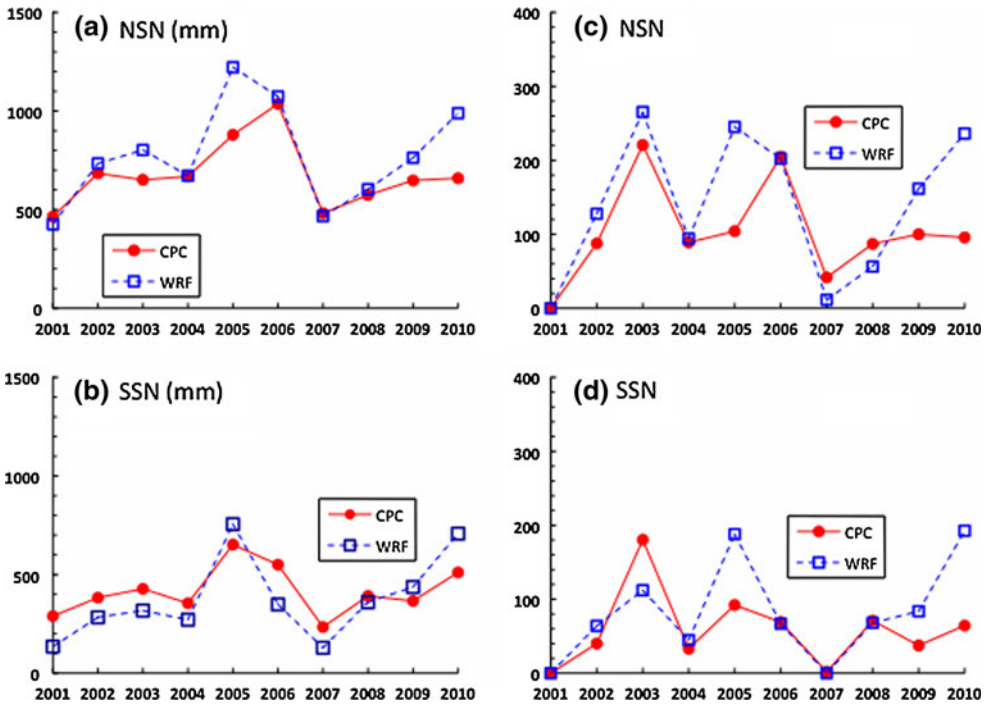

Fig. 8 The observed (CPC: *red solid line with solid circle*) and simulated (*blue dashed line with open square*) season-total (**a**, **b**) and AR-total (**c**, **d**) precipitation in the southern (SSN) and northern (NSN) Sierra Nevada regions for the 10 WYs 2001–2010

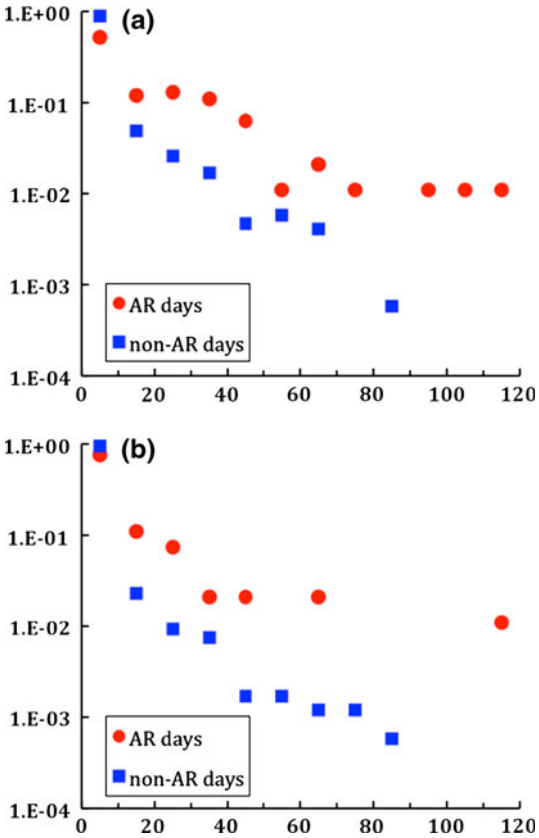

Fig. 9 The PDF of the simulated daily precipitation for the AR (*red*) and non-AR (*blue*) days in the **a** southern (SSN) and **b** northern (NSN) Sierra Nevada regions for the 10 WYs 2001–2010

landfall. Because consecutive days of AR landfalls are counted as separate AR days in both studies, the definition used in Dettinger et al. (2011) will systematically overestimate AR precipitation by double counting AR precipitation for the cases of consecutive-day AR landfalls. The definition used in this study will systematically underestimate AR precipitation by not counting the precipitation occurred after 00UTC in the case AR landfall starts on the concurrent day and ends in the following day. Another source of the differences between the two estimates is the presence (in Dettinger et al.) or absence (this study) of post-AR precipitation in the AR-precipitation estimates. Thus the true contribution of AR landfalls to the cold season precipitation will be between the estimates by Dettinger et al. (2011) and this study.

Overall, ARs affect the northern California region more than the southern region in both the amount and intensity of cold season precipitation. The differences in the AR effects between the northern and southern California found in this study are not likely to be attributed to the differences in the number of ARs as nearly the same number of AR landfalls have occurred in the northern and southern coasts over the entire analysis period. Instead, the north–south contrast may be related with the fact that winter storm tracks are more active for northern California and/or the southerly low-level moisture transport associated with the blocking by the coastal range and the Sierra Nevada.

For the Sierra Nevada region, the number of ARs is only marginally correlated with the cold-season precipitation totals. The AR storms are much more clearly related with the occurrence of heavy precipitation events as found by Neiman et al. (2008b) and for snow accumulation by Guan et al. (2010). The freezing level altitudes are also higher for AR storms than non-AR storms by 414 and 421 m in the NSN and SSN regions respectively, corresponding to higher low-level temperatures during the AR storms. The warmer low atmosphere during AR storms that often accompanies rainfall on existing snowpack, can promote snowmelt in high elevation regions (Neiman et al. 2008b). Because of these large precipitation intensity and snowmelt during AR storms, AR landfalls are of a particular concern for the occurrence of high river stages in California as shown by Dettinger et al. (2011).

Evaluation of the cold season simulations over the 10 WYs shows that the WRF model can reasonably simulate the differences in the precipitation and freezing level altitudes during AR- and non-AR storms. The observed contrast in the seasonal precipitation totals as well as the percentage of the season-total precipitation from AR storms between the northern and southern California regions are well simulated by the WRF model. In addition, the differences in the PDF of daily precipitation intensity and freezing-level altitudes between the AR and non-AR storms are reasonably simulated. The results of model evaluation suggests that the WRF model possesses useful skill in simulating the characteristics of precipitation and low-tropospheric temperatures in California, especially in the hydrologically important Sierra Nevada regions, over seasonal time scales.

Acknowledgments The CPC precipitation data were obtained the NOAA/OAR/ESRL PSD from its Web site http://www.esrl.noaa.gov/psd/. We thank Wei Shi for discussions on the CPC data. The ERA-Interim data were obtained from the ECMWF data distribution portal http://data-portal.ecmwf.int/data/d/license/interim/. This study is supported by NASA ARRA, NASA Energy and Water Cycle Study, NASA NCA (ID 11-NCA11-0028), the UC Lab 'Enhancing California's water resources management system', and NSF EaSM (ID 2011-67004-30224) and ExArch (ID 1125798) projects. The contribution from Duane E. Waliser, Bin Guan, and Ju-Mee Ryoo to this study was performed on behalf of the Jet Propulsion Laboratory, California Institute of Technology, under a contract with the National Aeronautics and Space Administration.

References

Bao J, Michelson SA, Neiman PJ, Ralph FM, Wilczak JM (2006) Interpretation of enhanced integrated water vapor bands

associated with extratropical cyclones: their formation and connection to tropical moisture. Mon Weather Rev 134:1063–1080

Dettinger M (2004) Fifty-two years of pineapple-express storms across the west coast of North America. California Energy Commission PIER Energy-Related Environmental Research report CEC-500-2005-004. California Energy Commission, Sacramento, CA, USA, p 15

Dettinger M, Ralph FM, Das T, Neiman PJ, Cayan D (2011) Atmospheric rivers, floods, and the water resources of California. Water 3:445–478. doi:10.3390/w3020445

Giorgi F, Hurrell JW, Marinucci MR, Beniston M (1997) Elevation-dependency of the surface climate signal: a model study. J Clim 10:288–296

Guan B, Molotch NP, Waliser DE, Fetzer EJ, Neiman PJ (2010) Extreme snowfall events linked to atmospheric rivers and surface air temperature via satellite measurements. Geophys Res Lett 37:L20401. doi:10.1029/2010GL044696

Higgins RW, Shi W, Yarosh E (2000) Improved United States precipitation quality control system and analysis. NCEP/Climate Prediction Center Atlas, **7**, National Centers for Environmental Prediction

Kim J (1997) Precipitation and snow budget over the southwestern United States during the 1994–1995 winter season in a mesoscale model simulation. Water Resour Res 33:2831–2839

Kim J, Kang H (2007) The impact of the Sierra Nevada on low-level winds and water vapor transport. J Hydrometeorol 8:790–804

Kim J, Lee J-E (2003) A multi-year regional climate hindcast for the western US using the Mesoscale Atmospheric Simulation (MAS) model. J Hydrometeorol 4:878–890

Kim J, Kim T-K, Arritt RW, Miller NL (2002) Impacts of increased atmospheric CO_2 on the hydroclimate of the western United States. J Clim 15:1926–1942

Knippertz P, Wernli H (2010) A Lagrangian climatology of tropical moisture exports to the northern hemispheric extratropics. J Clim 23:987–1003

Leung LR, Qian Y (2009) Atmospheric rivers induced heavy precipitation and flooding in the western US simulated by the WRF regional climate model. Geophys Res Lett 36:L03820. doi:10.1029/2008GL036445

Nature (2010) Validation required. Nature 463. doi:10.1038/463849a

Neiman PJ, Ralph FM, Wick GA, Kuo Y, Lee T, Ma Z, Taylor GH, Dettinger MD (2008a) Diagnosis of an intense atmospheric river impacting the Pacific Northwest: storm summary and offshore vertical structure observed with COSMIC satellite retrievals. Mon Weather Rev 136:4398–4420

Neiman PJ, Ralph FM, Wick GA, Lundquist J, Dettinger MD (2008b) Meteorological characteristics and overland precipitation impacts of atmospheric rivers affecting the West Coast of North America based on eight years of SSM/I satellite observations. J Hydrometeorol 9:22–47

Ralph FM, Neiman PJ, Wick GA (2004) Satellite and CALJET aircraft observations of atmospheric rivers over the eastern North Pacific Ocean during the winter of 1997/1998. Mon Weather Rev 132:1721–1745

Ralph FM, Neiman PJ, Wick GA, Gutman SI, Dettinger MD, Cayan DR, White AB (2006) Flooding on California's Russian river: the role of atmospheric rivers. Geophys Res Lett 36:L06812. doi:10.1029/2008GL037122

Ryoo J-M, Kim J, Fetzer EJ, Waliser DE (2010) A study of storm tracks and the cold season precipitation characteristics in California using trajectory model. AGU fall meeting, San Francisco, CA

Simmons A, Uppala S, Dee D, Kobayashi S (2006) ERA-Interim: new ECMWF reanalysis products from 1989 onwards. ECMWF Newsletter No. 110-Winter 2006/2007, pp 25–35. [http://www.ecmwf.int/publications/newsletters]

Skamarock WC, Klemp JB, Dudhia J, Gill DO, Baker DM, Duda MG, Huang X, Wang W, Powers JG (2008) A description of the advanced research WRF version 3. NCAR/TN-475+STR, NCAR technical note, June 2008

Soong S, Kim J (1996) Simulation of a heavy precipitation event in California. Clim Change 32:55–77

Zhu Y, Newell RE (1994) Atmospheric rivers and bombs. Geophys Res Lett 21:1999–2002

Zhu Y, Newell RE (1998) A proposed algorithm for moisture fluxes from atmospheric rivers. Mon Weather Rev 126:725–735